

Synthesis of New Heteroleptic Iridium(III) Complex Consisting of 2-Phenylquinoline and 2-[4-(Trimethylsilyl)phenyl]Pyridine for Red and White Organic Light-Emitting Diodes

Hee Un Kim¹, Jae-Ho Jang¹, Hea Jung Park¹, Jun Yeob Lee², and Do-Hoon Hwang^{1,*}

¹Department of Chemistry, and Chemistry Institute for Functional Materials, Pusan National University, Busan 609-735, Republic of Korea

²School of Chemical Engineering, Sungkyunkwan University 2066, Seobu-ro, Jangan-gu, Suwon, Gyeonggi 440-746, Republic of Korea

A novel red iridium(III) complex, (PQ)₂Ir(TMSppy), containing 2-phenylquinoline (PQ) as the main cyclometalated ligand and 2-[4-(trimethylsilyl)phenyl]pyridine (TMSppy) as the ancillary ligand, was synthesized for use in phosphorescent organic light-emitting diodes (OLEDs). (PQ)₂Ir(TMSppy) had a red emission with a maximum emission wavelength (λ_{max}) at 603 nm. To investigate the (PQ)₂Ir(TMSppy) as a red emitter in OLEDs, we fabricated a device with a multi-layer architecture. The (PQ)₂Ir(TMSppy) device showed an electroluminescence (EL) maximum emission peak at 612 nm and showed a maximum quantum efficiency (EQE_{max}) of 15.5% at a 10% doping concentration. In addition, white OLEDs, having three primary color components, made from (PQ)₂Ir(TMSppy) with bis(4,6-difluorophenylpyridine)picolinate (Flrpic) and tris(2-phenylpyridinato-C²,N)iridium(III) (Ir(ppy)₃) gave the best performances, with an EQE_{max} of 18.1%, maximum power efficiency (PE_{max}) of 22.8 lm/w, and maximum current efficiency (CE_{max}) of 36.5 cd/A with Commission Internationale de L'Eclairage coordinates of (0.39, 0.42) at a luminance of 1,000 cd/m².

Keywords: Phosphorescence, Iridium(III) Complex, Organic Light-Emitting Diodes.

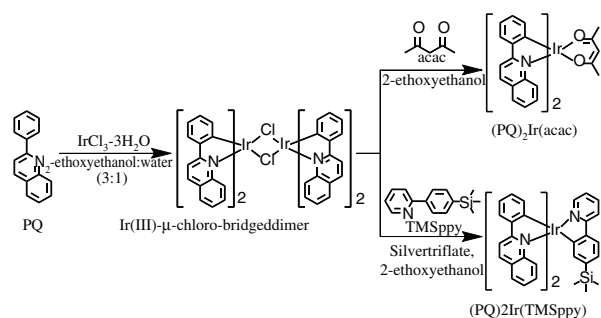
1. INTRODUCTION

Organic light-emitting diodes (OLEDs) have attracted great attention during the last two decades, particularly for applications such as full-color and flat-panel displays. In these fields, OLEDs have many remarkable advantages, such as low operating voltages for low power consumption, high contrast and brightness with a wide viewing angle, faster response times than liquid-crystal displays (LCDs), and a light weight for flexible displays and solid state lighting applications.¹⁻⁴ White OLEDs (WOLED), using the three primary colors of OLEDs technique, are ideal candidates for potentially cost-effective, environmentally friendly, solid-state lighting sources. Thus, applications of the OLEDs technique are becoming diverse.^{5,6}

Phosphorescent OLEDs based on complexes containing Ir(III), Pt(II), Os(II), and Ru(II) as typical heavy metals,

can achieve a theoretical internal quantum efficiency of 100%, due to generating light from both singlet and triplet excitons by intersystem crossing.⁷⁻¹³ Among the heavy metal complexes, iridium(III) complexes have been employed in many phosphorescent emitters, such as homoleptic [(C[^]N)₃Ir, CN; cyclometalated ligand] or heteroleptic [(C[^]N)₂Ir(LX), LX; ancillary ligand] complexes. These iridium(III) complexes exhibit good photo and thermal stability, high photoluminescence (PL) quantum efficiency (Φ_{PL}), and relatively short excited-state lifetimes in the microsecond range.^{14,15} In particular, heteroleptic iridium(III) complexes can modify ancillary ligands as well as cyclometalated ligands, which has the advantages of easy control of photophysical and electrochemical properties, and electroluminescent (EL) performance. Typical ancillary ligands in heteroleptic iridium(III) complexes are picolinic acid (pic), acetylacetonate (acac), and 2,2,6,6-tetramethylheptane-3,5-dione (tmd), and these have been the most widely used until

* Author to whom correspondence should be addressed.



Scheme 1. Synthetic routes for $(PQ)_2Ir(TMSppy)$.

now.^{16–18} In particular, acac is currently the most widely used ancillary ligand in red-phosphorescent emitters, such as bis(2-phenylquinoline)(acetylacetonate)iridium(III) $[(pq)_2Ir(acac)]$, with excellent color purity.¹⁹ However, acac as an ancillary ligand in heteroleptic iridium(III) complexes causes decreased OLEDs performances due to intrinsic problems such as low thermal stability and concentration self-quenching or triplet–triplet annihilation at high doping concentrations in phosphorescent OLEDs.^{20,21} To solve these problems, structural modifications of various ligands in iridium(III) complexes to prevent self-quenching have been suggested. Lee et al. reported a *fac*-tris(2-phenylpyridine)iridium(III) $[Ir(ppy)_3]$ derivative containing a bulky pinene group in 2-phenylpyridine (ppy).²² The bulky pinene group in the iridium(III) complex lead to minimum bimolecular interaction and, therefore, significantly reducing self-quenching at very high doping concentration by sterically hindered the pinene spacers.

In this paper, we have designed an iridium(III) complex $[(PQ)_2Ir(TMSppy)]$ based on 2-phenylquinoline (PQ) as the main cyclometalated ligand and 2-[4-(trimethylsilyl)phenyl]pyridine (TMSppy) as a new ancillary ligand. $(PQ)_2Ir(TMSppy)$ was able to reduce concentration self-quenching at high doping concentrations and improve EL performance in phosphorescent OLEDs due to the introduction of the bulky TMSppy moiety. The ppy core in TMSppy has a high thermal stability, high phosphorescence (PL) quantum yield, and a broad-band full width at half maximum (FWHM) range of emission.²³ Moreover, the sterically bulky trimethylsilyl group in TMSppy is electron donating, chemical stable and have good solubility. The synthetic routes and chemical structures of the heteroleptic iridium complexes are outlined in Scheme 1.

2. EXPERIMENTAL DETAILS

2.1. Materials

Phenylboronic acid, 2-chloroquinoline, 2-(4-bromophenyl)pyridine, trimethylsilyl chloride, tetrakis(triphenylphosphine)palladium(0), iridium(III) chloride hydrate, and silver trifluoromethanesulfonate were purchased from Aldrich and Alfa Aesar. All chemicals were used without further purification.

2.2. Synthesis of Red Iridium(III) Complex

2-Phenylquinoline (PQ), 2-(4-(trimethylsilyl)phenyl)pyridine (TMSppy), and Ir(III)- μ -chloro-bridged dimer $[(Ir(PQ)_2IrCl)_2]$ were synthesized in similar ways according to the methods described in previous reports.⁷

2.2.1. Synthesis of 2-Phenylquinoline (PQ)

2-Chloroquinoline (5.0 g, 30.6 mmol), phenylboronic acid (4.47 g, 36.7 mmol), and tetrakis(triphenylphosphine)palladium(0) (1.01 g, 0.92 mmol) were dissolved in THF. A solution of 2 M K_2CO_3 (100 ml) and Aliquat 336 (1.23 g, 3.06 mmol) was added, and the mixture was refluxed overnight under a nitrogen atmosphere. The reaction mixture was cooled to room temperature and extracted with ethyl acetate. The organic layer was washed with water and dried over $MgSO_4$. The solvent was removed under reduced pressure to give a crude residue. The crude product was purified by column chromatography on silica gel to obtain PQ (5.11 g, 81.5%). 1H NMR (300 MHz, $CDCl_3$) δ (ppm): 8.30 (*d*, 1H), 8.24 (*d*, 2H), 8.11 (*d*, 1H), 7.82 (*m*, 3H), 7.59 (*m*, 4H). ^{13}C NMR (75 MHz, $CDCl_3$) δ (ppm): 157.39, 136.84, 129.75, 129.71, 129.36, 128.88, 128.16, 127.62, 127.49, 127.22, 127.20, 126.33, 119.04.

2.2.2. Synthesis of 2-(4-(trimethylsilyl)phenyl)pyridine (TMSppy)

Under a nitrogen atmosphere, *n*-BuLi (7.7 ml, 15.4 mmol, 2.0 M solution in hexane) was added dropwise to 2-(4-bromophenyl)pyridine (3.0 g, 12.8 mmol) in THF at -78 °C. The mixture was stirred at -78 °C for 1 h, and then chlorotrimethylsilane (2.45 ml, 19.2 mmol) was added in one portion. The reaction mixture was allowed to warm to room temperature overnight. After the reaction mixture was quenched with methanol, it was extracted with ethyl acetate and the organic layer was washed with water and dried over $MgSO_4$. The solvent was removed under reduced pressure to give a crude residue. The crude product was purified by column chromatography on silica gel to obtain TMSppy (1.86 g, 63.7%). 1H NMR (300 MHz, $CDCl_3$) δ (ppm): 7.75 (*d*, 1H), 7.99 (*d*, 2H), 7.73 (*m*, 2H), 7.65 (*d*, 2H), 7.22 (*m*, 1H), 0.30 (*s*, 9H, CH_3). ^{13}C NMR (75 MHz, $CDCl_3$) δ (ppm): 157.45, 149.72, 141.41, 139.70, 136.71, 133.80, 126.13, 122.16, 120.58, 1.08.

2.2.3. Synthesis of Ir(III)- μ -Chloro-Bridged Dimer $[(Ir(PQ)_2IrCl)_2]$

The cyclometalated iridium(III)- μ -chloro-bridged dimer complex $[Ir(PQ)_2Cl]_2$, which was used directly in the next step without further purification.

2.2.4. Synthesis of $(PQ)_2Ir(TMSppy)$

$(PQ)_2Ir(TMSppy)$ was synthesized similarly with the previous reports.^{24,25} The $[Ir(PQ)_2Cl]_2$ dimer complex

(0.5 g, 0.39 mmol) and silver trifluoromethanesulfonate (0.21 g, 0.83 mmol) were placed in a 100 mL round-bottomed flask with acetonitrile (30 mL) and the mixture was refluxed for 6 h. After cooling, the deep-red solution was filtered to remove insoluble materials and the solvent was removed in vacuo. TMSppy (0.20 g, 0.88 mmol) and 2-ethoxyethanol (30 mL) were added to the resulting solid, $[\text{Ir}(\text{PQ})_2(\text{CH}_3\text{CN})_2]^+$ trifluoromethanesulfonate], and the mixture was refluxed under a nitrogen atmosphere for 12 h. After cooling to room temperature, the crude solution was poured into water, extracted with dichloromethane and brine, dried over MgSO_4 , and concentrated in vacuo. The residue was purified using column chromatography with dichloromethane as the eluent. The resulting solid was recrystallized from dichloromethane and methanol, and then the red solid was dried in vacuo. $(\text{PQ})_2\text{Ir}(\text{TMSppy})$ was obtained as a red solid (0.17 g, 53.6%). ^1H NMR (300 MHz, CDCl_3) δ (ppm): 8.26 (*d*, 1H), 8.17 (*m*, 3H), 7.97 (*m*, 3H), 7.64 (*m*, 4H), 7.57 (*d*, 1H), 7.47 (*t*, 1H), 7.29 (*d*, 1H), 7.21 (*m*, 1H), 6.94 (*m*, 4H), 6.77 (*m*, 8H), 0.02 (*s*, 9H). ^{13}C NMR (75 MHz, CDCl_3) δ (ppm): 167.56, 166.12, 163.43, 160.90, 156.62, 149.15, 148.38, 147.82, 146.44, 146.23, 143.57, 141.50, 139.18, 137.25, 137.11, 136.57, 136.39, 135.67, 130.03, 129.60, 129.20, 128.68, 128.59, 128.07, 127.67, 127.58, 127.04, 126.02, 125.90, 125.60, 124.93, 124.72, 121.91, 120.15, 119.84, 118.70, 118.14, 117.98, 77.46, 77.03, 76.62, 1.30. Anal. Calcd (%) for $\text{C}_{44}\text{H}_{36}\text{IrN}_3\text{Si}$: C; 63.90, H; 4.39, N; 5.08. Found: C; 63.84, H; 4.41, N; 5.11. MALDI-TOF (M^+ , $\text{C}_{44}\text{H}_{36}\text{IrN}_3\text{Si}$): calcd; 827.23, found; 827.35. (Purity: 99.7%, by HPLC). T_d (5% weight loss): 407 °C.

2.3. Measurements and Device Fabrication

Measurements and devices fabrication were performed in similar ways according to the methods described in previous report.⁷

3. RESULTS AND DISCUSSION

3.1. Photophysical Properties

Figure 1 shows the UV-visible absorption and phosphorescence (PL) spectra of $(\text{PQ})_2\text{Ir}(\text{TMSppy})$ in both toluene solution and the neat solid state at 298 K. The absorption bands at approximately 290–350 nm and weaker absorption bands in the region above 390 nm, which corresponded to the spin allowed $\pi-\pi^*$ transitions of the cyclometalated main ligand, and spin-allowed admixture of singlet and triplet metal-to-ligand charge transfer ($^1\text{MLCT}$, $^3\text{MLCT}$) transitions, respectively. These MLCT bands were attributed to effective mixing between the ligand $^3\pi-\pi^*$ state and spin-forbidden $^3\text{MLCT}$, and the higher-lying $^1\text{MLCT}$ transitions induced by strong spin-orbit coupling effects. The optical energy bandgap of $(\text{PQ})_2\text{Ir}(\text{TMSppy})$ was calculated to be 2.16 eV.

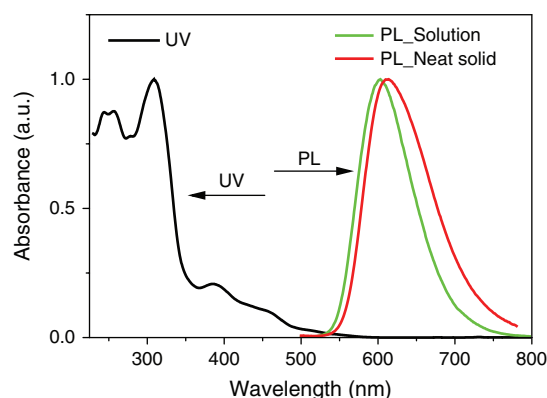


Figure 1. UV-visible absorption and PL spectra of $(\text{PQ})_2\text{Ir}(\text{TMSppy})$ in solution and neat solid film state at 298 K.

The maximum PL emission wavelength (λ_{max}) of $(\text{PQ})_2\text{Ir}(\text{TMSppy})$ in toluene solution at 298 K was observed at 603 nm. This value was red-shifted compared to that of a typical iridium(III) complex containing acac, $(\text{PQ})_2\text{Ir}(\text{acac})$ (598 nm at 298 K). Also, a red-shift of the λ_{max} from solution to neat solid state in $(\text{PQ})_2\text{Ir}(\text{TMSppy})$ (614 nm) was observed, which may be related to aggregation effects between the iridium(III) complexes.

The PL quantum yields (Φ_{PL}) of $(\text{PQ})_2\text{Ir}(\text{TMSppy})$ in dilute degassed 2-methyltetrahydrofuran solution (10^{-5} M) was measured using $(\text{PQ})_2\text{Ir}(\text{acac})$ as a standard. The solution state of Φ_{PL} for $(\text{PQ})_2\text{Ir}(\text{TMSppy})$ was calculated to be 0.13. The Φ_{PL} of $(\text{PQ})_2\text{Ir}(\text{TMSppy})$ was slightly higher than that of $(\text{PQ})_2\text{Ir}(\text{acac})$ as a standard ($\Phi_{\text{PL}} = 0.10$).²⁶

3.2. Theoretical Calculation

To further understand the effects of TMSppy on the iridium(III) complex, we performed density functional theory (DFT) calculations using B3LYP/6-31G(d) basis sets.²⁷ As shown in Figure 2, the highest occupied molecular orbital (HOMO) of $(\text{PQ})_2\text{Ir}(\text{TMSppy})$ was mainly

Complex	$(\text{PQ})_2\text{Ir}(\text{acac})$	$(\text{PQ})_2\text{Ir}(\text{TMSppy})$
	$E = -1.93\text{ eV}$	$E = -1.91\text{ eV}$
LUMO		
HOMO		
	$E = -5.02\text{ eV}$	$E = -4.94\text{ eV}$

Figure 2. Calculated HOMO and LUMO of $(\text{PQ})_2\text{Ir}(\text{TMSppy})$ using DFT at the B3LYP/6-31G(d) level.

Table I. Summary of performances of red-phosphorescent OLEDs.

Dopant	$x\%$	λ_{\max} (nm)	CIE ^a (x, y)	V_i (V)	L_{\max} (cd/m ²)	EQE ^b (%)	LE ^b (cd/A)	PE ^b (lm/W)
(PQ) ₂ Ir(TMSppy)	3	600	(0.59, 0.41)	3.0	12,204	15.1/14.2	27.5/26.0	28.8/21.0
	5	603	(0.60, 0.40)	3.0	21,911	14.5/14.2	24.8/24.2	23.7/18.9
	10	611	(0.61, 0.39)	3.0	29,092	15.5/15.1	24.1/23.5	25.1/18.4
(PQ) ₂ Ir(acac)	5	597	(0.59, 0.39)	3.5	10,450	14.9/13.9	22.3/21.1	15.0/9.7

Notes: ^aValues measured at a luminance of 1,000 cd/m². ^bValues measured at maximum efficiency and luminance of 1,000 cd/m².

localized at the phenyl group in PQ, the *d*-orbital of the iridium atom, and the phenyl unit in TMSppy, whereas the lowest unoccupied molecular orbital (LUMO) was largely located on the quinolone unit in PQ. In general, typical ancillary ligands, such as acac, do not contribute to both the HOMO and LUMO in iridium(III) complexes. Interestingly, TMSppy in (PQ)₂Ir(TMSppy) contributed to the HOMO of the iridium(III) complex. The HOMO and LUMO energy levels of (PQ)₂Ir(TMSppy) were -4.94 and -1.91 eV, respectively. The calculated HOMO and LUMO energy levels of the iridium(III) complex with TMSppy were slightly higher than those of the iridium(III) complex containing acac (HOMO = -5.02 eV, LUMO = -1.93 eV).

3.3. Electrochemical Properties

The electrochemical behavior of (PQ)₂Ir(TMSppy) was determined by cyclic voltammetry (CV). The HOMO energy level, calculated from onset oxidation

potential, was -5.08 eV. The HOMO energy level of (PQ)₂Ir(TMSppy) was higher than in the well-known (PQ)₂Ir(acac) complex (HOMO = -5.22 eV). The LUMO energy level was calculated from differences between the HOMO energy level and the optical bandgap energy. The LUMO energy level of (PQ)₂Ir(TMSppy) was -2.93 eV. These HOMO and LUMO energy levels are consistent with DFT calculated energy levels.

3.4. Electrophosphorescent OLEDs

To investigate (PQ)₂Ir(TMSppy) as a dopant in red-phosphorescent OLEDs, we fabricated a device with a multi-layer architecture containing ITO (50 nm)/PEDOT:PSS (40 nm)/NPB (20 nm)/TCTA (10 nm)/TCTA:TPBi:(PQ)₂Ir(TMSppy) (25 nm, $x\%$)/TPBi (35 nm)/LiF (1 nm)/Al (200 nm). The TCTA:TPBi (1:1)

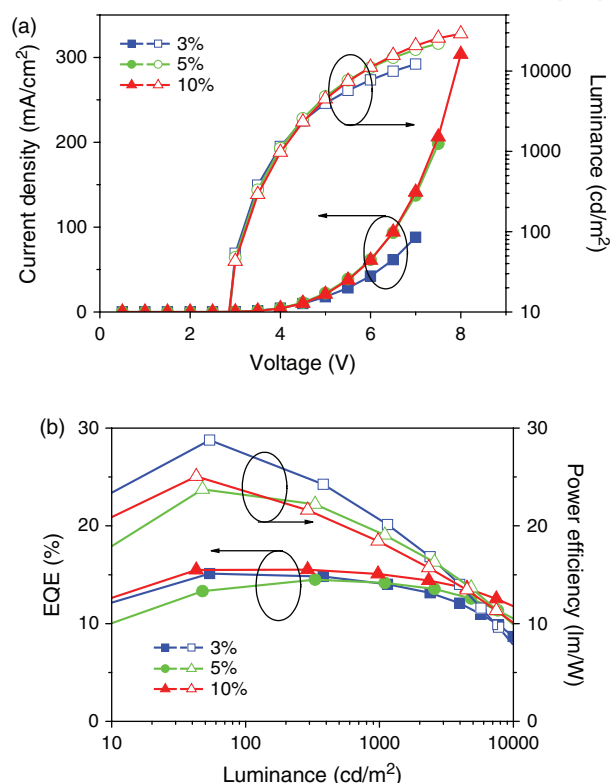


Figure 3. (a) *I*-*V*-*L* and (b) EQE-*L*-CE curves of red OLED.

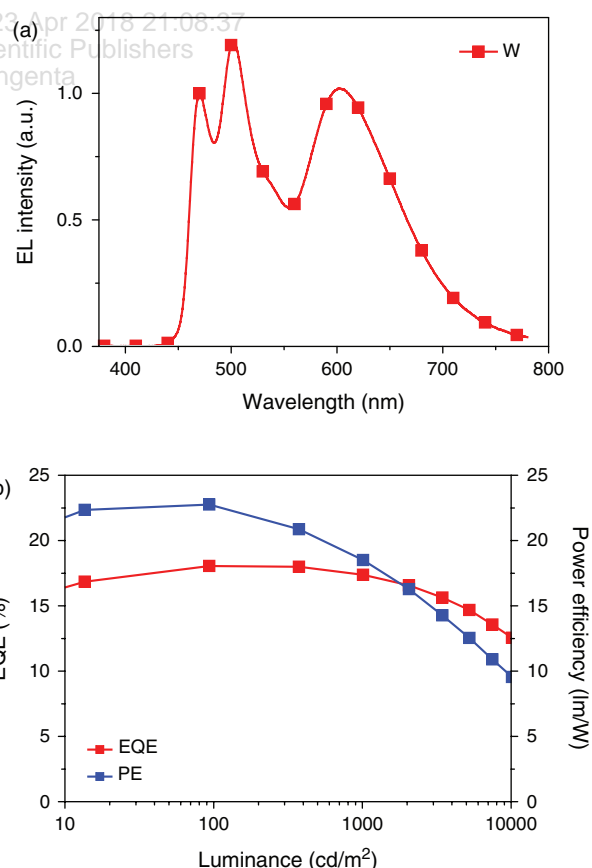


Figure 4. (a) EL spectra and (b) EQE-*L*-PE curves of WOLED.

Table II. Summary of performances of WOLED.

WOLED	V_t (V)	L_{\max} (cd/m ²)	EQE ^a (%)	LE ^a (cd/A)	PE ^a (lm/W)	CIE ^b (x, y)	CCT ^b (K)
	4.0	27,232	18.1/17.4	36.5/35.3	22.8/18.5	(0.39, 0.42)	3,996

Notes: ^aValues measured at maximum efficiency and luminance of 1,000 cd/m². ^bValues measured at a luminance of 1,000 cd/m².

mixture was used as a mixed-host system for efficient hole and electron injection. The device performances of red-phosphorescent OLEDs were optimized by changing the doping concentration (3%, 5%, and 10%) of (PQ)₂Ir(TMSppy). The various doping concentrations and detailed characteristics of (PQ)₂Ir(TMSppy) are summarized in Table I.

The maximum emission peaks for a 3, 5, and 10% doping concentration for (PQ)₂Ir(TMSppy) appeared at 600, 603, and 611 nm, respectively. The maximum emission peaks of (PQ)₂Ir(TMSppy) were slightly red-shifted as the doping concentration increased from 3% to 10%, because of the increased aggregation of dopant in the devices at higher doping concentrations. The red-shift in maximum emission peaks at high doping concentrations of (PQ)₂Ir(TMSppy) were consistent with the aggregation effects on (PQ)₂Ir(TMSppy) neat solid films. The corresponding Commission Internationale de L'Éclairage (CIE) coordinates of (PQ)₂Ir(TMSppy) were (0.59, 0.41) for 3%, (0.60, 0.40) for 5%, and (0.61, 0.39) for 10% at a luminance of 1,000 cd/m².

The current density–voltage–luminance (I – V – L) curves of (PQ)₂Ir(TMSppy) are shown in Figure 3(a). The current density of the OLEDs increased with increasing concentration of the (PQ)₂Ir(TMSppy) dopant, due to improved charge hopping at higher doping concentrations.²⁸ The turn-on voltage (V_t , defined as the bias at a luminance of 1 cd/m²) of all devices was 3.0 V, and the driving voltage (V_d , defined as the bias at a luminance of 1,000 cd/m²) of the devices was 3.8 V at 3%, 3.9 V at 5%, and 4.1 V at 10% doping, respectively. In addition, the maximum luminance (L_{\max}) of (PQ)₂Ir(TMSppy) was 12,204 cd/m² at 3%, 21,911 cd/m² at 5%, and 29,092 cd/m² at 10% doping, respectively.

Figure 3(b) shows the external quantum efficiency–luminance–power efficiency (EQE–L–PE) curves of (PQ)₂Ir(TMSppy). The external quantum efficiency of (PQ)₂Ir(TMSppy) was optimized at the 10% dopant concentration and the maximum external quantum efficiency (EQE_{max}) was 15.5%, slightly higher than that of (PQ)₂Ir(acac) (EQE_{max} = 14.9% at 5% doping concentration). Also, the EQE value at a luminance of 1,000 cd/m² for (PQ)₂Ir(TMSppy) at a 10% doping concentration was 15.1%. The EQE value of (PQ)₂Ir(TMSppy) had a low efficiency roll-off with increasing luminance. These results could be due to the sterically hindered trimethylsilyl group in TMSppy preventing concentration self-quenching at high doping concentrations and reducing triplet–triplet annihilation in the OLEDs.²⁹ The optimized

maximum power efficiency (PE_{max}) of (PQ)₂Ir(TMSppy) was 28.8 lm/W at a 3% doping concentration. The low driving voltage of (PQ)₂Ir(TMSppy) at a 3% doping concentration improved the PE value of the OLEDs.

We fabricated a primary three-color component WOLED that incorporated bis[2-(4,6-difluorophenyl)pyridinato-C²,N](picolinato)iridium(III) [Flrpic] as the blue emitter, Ir(ppy)₃ as the green emitter, and (PQ)₂Ir(TMSppy) as the red emitter with different doping concentrations. EL spectra of the W device containing (PQ)₂Ir(TMSppy) are shown in Figure 4(a). The white EL spectra showed blue, green, and red peaks at 470, 502, and 602 nm, respectively; these matched well with the peak wavelengths of Flrpic, Ir(ppy)₃, and (PQ)₂Ir(TMSppy), respectively. The CIE color coordinate and correlated color temperature (CCT) value for the W device were (0.39, 0.42) and 3996 K, respectively, at a luminance of 1,000 cd/m².

The EQE–L–PE curves for the W device containing (PQ)₂Ir(TMSppy) are shown in Figure 4(b), with the detailed characteristics summarized in Table II. The V_t and L_{\max} values of the W device were 4.0 V and 27,232 cd/m², respectively. The EQE_{max} and EQE for the W device at a luminance of 1,000 cd/m² were 18.1% and 17.4%, respectively, representing a low efficiency roll-off with increasing luminance. Additionally, maximum current efficiency (CE_{max}) and PE_{max} values for the W device were 36.5 cd/A and 22.8 lm/W, respectively. An EQE_{max} value of 18.1% was obtained for the device with the structure TAPC/mCP/mCP:Flrpic:Ir(ppy)₃/TCTA:TPBi:(PQ)₂Ir(TMSppy)/TSPO1/TPBi. In particular, the exciton blocking layer (TSPO1) in the W device structure improved both the electron injection and charge balance of the emitting layer to give a high external quantum efficiency WOLED.²⁶ Also, we measured EL spectra and CIE color coordinates for the fabricated W

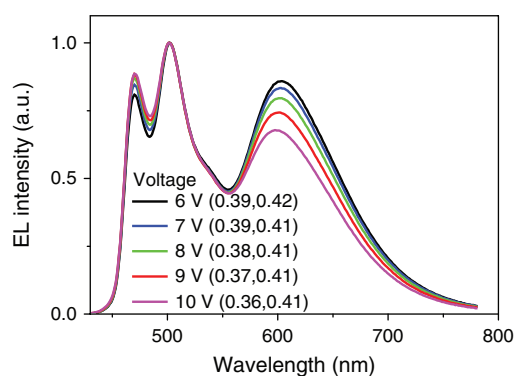


Figure 5. (a) EL spectra of W device at different driving voltages.

device at different driving voltages, from 6 to 10 V, to test the color stability; the results are shown in Figure 5. Despite the intensity of the red emission region in the spectrum showing a slight decrease relative to the blue and green regions, the CIE color coordinates of the device were not significantly changed.

4. CONCLUSION

In conclusion, we synthesized a $(PQ)_2Ir(TMSpy)$ and investigated its application as a red dopant in phosphorescent OLEDs. The luminance and external quantum efficiency of the $(PQ)_2Ir(TMSpy)$ device at 10% doping concentration in a red-phosphorescent OLEDs were higher than that of the corresponding iridium(III) complex containing acac. The maximum luminance and external quantum efficiency of the device fabricated using $(PQ)_2Ir(TMSpy)$ were 29,092 cd/m^2 and 15.5%, respectively. The improved luminance and quantum efficiency for $(PQ)_2Ir(TMSpy)$ were attributed to TMSpy in the iridium(III) complex, because the sterically bulky substituent could effectively reduce concentration self-quenching and triplet-triplet annihilation at high doping concentrations. Also, the EQE_{max} and EQE at a luminance of 1,000 cd/m^2 in the WOLED with $(PQ)_2Ir(TMSpy)$ were 18.1 and 17.4%, respectively. The EQE curves of the WOLED with $(PQ)_2Ir(TMSpy)$ showed a low efficiency roll-off with increasing luminance. Therefore, TMSpy is a good candidate as an ancillary ligand for heteroleptic iridium(III) complexes.

Acknowledgment: This research was supported by the Ministry of Trade, Industry and Energy (MOTIE, Korea) under Industrial Technology Innovation Program No. 10067715 and a National Research Foundation (NRF) grants funded by the Korean Government (NRF-2014R1A2A2A01007318).

References and Notes

- M. A. Baldo, D. F. O'Brien, Y. You, A. Shoustikov, S. Sibley, M. E. Thompson, and S. R. Forrest, *Nature* 395, 151 (1998).
- S. R. Forrest, *Nature* 428, 911 (2004).
- J. Y. Lee, *J. Inf. Disp.* 15, 139 (2014).
- T.-H. Han, S.-H. Jeong, Y. Lee, H.-K. Seo, S.-J. Kwon, M.-H. Park, and T.-W. Lee, *J. Inf. Disp.* 16, 71 (2015).
- B. D'Andrade, *Nat. Photonics* 1, 33 (2007).
- H. Sasabe and J. Kido, *J. Mater. Chem. C* 1, 1699 (2013).
- H. U. Kim, J.-H. Jang, W. Song, B. J. Jung, J. Y. Lee, and D.-H. Hwang, *J. Mater. Chem. C* 3, 12107 (2015).
- W. Lu, B.-X. Mi, M. C. W. Chan, Z. Hui, C.-M. Che, N. Zhu, and S.-T. Lee, *J. Am. Chem. Soc.* 126, 4985 (2004).
- M. Cocchi, D. Virgili, V. Fattori, D. L. Rochester, and J. A. G. Williams, *Adv. Funct. Mater.* 17, 285 (2007).
- C.-M. Che, S.-C. Chan, H.-F. Xiang, M. C. W. Chan, Y. Liu, and Y. Wang, *Chem. Commun.* 1484 (2004).
- S. Bernhard, X. Gao, G. G. Malliaras, and H. D. Abruña, *Adv. Mater.* 14, 433 (2002).
- Y.-L. Tung, S.-W. Lee, Y. Chi, Y.-T. Tao, C.-H. Chien, Y.-M. Cheng, P.-T. Chou, S.-M. Peng, and C.-S. Liu, *J. Mater. Chem.* 15, 460 (2005).
- Y.-L. Tung, S.-W. Lee, Y. Chi, L.-S. Chen, C.-F. Shu, F.-I. Wu, A. J. Carty, P.-T. Chou, S.-M. Peng, and G.-H. Lee, *Adv. Mater.* 17, 1059 (2005).
- C. Adachi, R. C. Kwong, P. Djurovich, V. Adamovich, M. A. Baldo, M. E. Thompson, and S. R. Forrest, *Appl. Phys. Lett.* 79, 2082 (2001).
- T. Tsuzuki, N. Shirasawa, T. Suzuki, and S. Tokito, *Adv. Mater.* 15, 1455 (2003).
- S. Lamansky, P. Djurovich, D. Murphy, F. Abdel-Razzaq, H.-E. Lee, C. Adachi, P. E. Burrows, S. R. Forrest, and M. E. Thompson, *J. Am. Chem. Soc.* 123, 4304 (2001).
- H. U. Kim, J.-H. Jang, F. Xu, J. Y. Lee, and D.-H. Hwang, *J. Nanosci. Nanotechnol.* 16, 2773 (2016).
- J.-H. Jang, M. J. Kim, H. U. Kim, S. B. Lee, J. Lee, and D.-H. Hwang, *J. Nanosci. Nanotechnol.* 16, 8580 (2016).
- C.-H. Yang, C.-C. Tai, and I.-W. Sun, *J. Mater. Chem.* 14, 947 (2004).
- S. Reineke, G. Schwartz, K. Walzer, M. Falke, and K. Leo, *Appl. Phys. Lett.* 94, 163305 (2009).
- M. A. Baldo, C. Adachi, and S. R. Forrest, *Phys. Rev. B* 62, 10967 (2000).
- H. Z. Xie, M. W. Liu, O. Y. Wang, X. H. Zhang, C. S. Lee, L. S. Hung, S. T. Lee, P. F. Teng, H. L. Kwong, H. Zheng, and C. M. Che, *Adv. Mater.* 13, 1245 (2001).
- M. A. Baldo, S. Lamansky, P. E. Burrows, M. E. Thompson, and S. R. Forrest, *Appl. Phys. Lett.* 75, 4 (1999).
- X. Ren, M. E. Kondakova, D. J. Giesen, M. Rajeswaran, M. Madaras, and W. C. Lenhart, *Inorg. Chem.* 49, 1301 (2010).
- A. S. Ionkin, W. J. Marshall, D. C. Roe, and Y. Wang, *Dalton Trans.* 2468 (2006).
- D. H. Kim, N. S. Cho, H.-Y. Oh, J. H. Yang, W. S. Jeon, J. S. Park, M. C. Suh, and J. H. Kwon, *Adv. Mater.* 23, 2721 (2011).
- Gaussian 09, Gaussian, Inc., Wallingford, CT (2009).
- J. Park, H. Oh, S. Oh, J. Kim, H. J. Park, O. Y. Kim, J. Y. Lee, and Y. Kang, *Org. Electron.* 14, 3228 (2013).
- K. S. Yook and J. Y. Lee, *Org. Electron.* 12, 1293 (2011).

Received: 27 May 2016. Accepted: 27 August 2016.